University of Twente

Advanced Organ Bioengineering and Therapeutics (AOT)

The effect of mechanical stiffness and the novel ITGA5 targeting peptide in fibroblast activation

BSc Biomedical Engineering

July 3, 2023

Author:
Remco Hoen
s2178540

Chairman:
Prof. Dr. J. Prakash

Supervisor:
K. P. Pednekar, MSc

Abstract

Cancer is one of the leading causes of death in the Netherlands. Pancreatic Ductal Adenocarcinoma is one of the most devastating cancers, with a 10-year survival rate of only 3%. PDAC is known to be a fibrotic tumor which results in a dense, stiff TME. The TME influences the efficacy of therapeutic agents extensively as the TME can function as physical barrier around the tumor. A large portion of the TME consists of cancer-associated fibroblasts (CAFs). CAFs can be characterised by their increased ECM protein production and up-regulated secretion of pro-tumorigenic factors. In PDAC, Pancreatic Stellate Cells (PSCs) largely fill the CAF population. Targeting and potentially inactivating CAFs could prove to positively influence cancer therapeutic efficacy. The key growth factor responsible for PSC recruitment and activation to CAF is Transforming Growth Factor-β. Mechanical stiffness has also been suggested to play a role in fibroblast activation. For fibroblasts, $\alpha 5\beta 1$ integrin is the key integrin that enables mechanosensing. Upon activation, integrins induce cytoskeleton assembly which activates the mechanotransductor effectors of the Hippo pathway: YAP/TAZ. YAP/TAZ activation is recognized by nuclear translocalization where it influences cell proliferation and differentiation. The novel therapeutic peptide, called CyAV3.3, targets the integrin alpha 5 (ITGA5) subunit. This study aims to gain knowledge about the effect of mechanical stiffness in fibroblast activation, and demonstrate the inhibiting capabilities of the novel CyAV3.3 peptide on fibroblast activation in different matrix stiffness conditions. This was examined by comparing mechanical stiffness mediated PSC activation in low (0.2 kPa) and high (32 kPa) matrix stiffness conditions. Furthermore, in the same matrix stiffness conditions, PSCs were treated with CyAV3.3 to investigate activation inhibition. αSMA-, ITGA5- and nuclear YAP/TAZ expression levels were assessed by immunofluorescence staining. The study found significant increase in αSMA expression for high matrix stiffness. The research also demonstrated CyAV3.3 mediated downregulation of αSMA in high matrix stiffness conditions for non-TGF-β treated PSCs. In addition, the inhibiting effect of CyAV3.3 was seen for ITGA5 in TGF-β mediated PSC activation as well. Despite limiting factors, the study offers insight in the effect of mechanical stiffness in PSC activation. Furthermore, the study contributes to previous findings that implicate the inhibiting effect of CyAV3.3 on PSC activation. These findings can prove useful for improving cancer therapeutic efficacy.

Contents

List of Figures

1 Introduction

1.1 Cancer and the tumor microenvironment

Cancer is one of the leading causes of death in the Netherlands. The Netherlands Comprehensive Cancer Organisation (IKNL) reported that cancer accounted for 124 Thousand new cases and about 46 Thousand deaths annually [1]. Traditional treatment methods are chemotherapy, radiotherapy and surgery. Modern technologies include e.g. hormone therapy, stem cell therapies and immunotherapy [2].

One theoretical issue that is starting to become more dominant in the field concerns the focus of many current therapeutic approaches. Current treatment options primarily target the fast-growing tumor, but mostly ignore the tumor microenvironment (TME) [3].

The TME differs from the ECM of normal tissues, mainly in the abnormal structure and function of blood vessels, heterogeneity, high stroma pressure, and varied tissue stiffness. An increase of fibrosis causes the TME to be denser and stiffer, which can function as a physical barrier around tumor cells [4]. Furthermore, it was previously found that the TME drastically influences the succes of therapeutic agents in penetration, distribution and metabolism. Next to that the TME produces signals that can positively or negatively impact the way tumor cells grow and migrate [3]. This makes the TME an interesting and field of study in cancer research.

1.2 Cancer-associated fibroblasts and Pancreatic Ductal Adenocarcinoma

Cancer-associated fibroblasts (CAFs) are a major TME component in many fibrotic tumors [5]. CAFs are the fibroblasts found in the stroma of human cancers and are critical for shaping the TME [6]. Fibroblasts have a spindle-shaped morphology and are part of the connective tissue components. Fibroblasts are generally quiescent but transition into myofibroblasts when activated [7][8]. Activation can occur through simulation by growth factors (e.g. Transforming Growth Factor-β). Additionally, fibronectin and mechanical stimuli such as tissue stiffness and topography also have a role in fibroblast activation [9][10]. Once activated, fibroblasts proliferate, show higher activity in the synthesis of the ECM (e.g. collagen and fibronectin), release cytokines and exert physical forces on its surrounding tissue (e.g. by contraction) [7]. Previous research has established that activated fibroblasts, myofibroblasts, can be identified by (increased) α-Smooth Muscle Actin (α-SMA) expression [8][9][11]. High α-SMA expression is connected to actin polymerization and stimulates contraction, and contractile force applied by fibroblasts. α-SMA is also highly expressed in smooth muscle cells [12][13].

CAFs differ from normal fibroblasts in their increased collagen and ECM protein production and up-regulated secretion of growth factors and cytokines [14]. These factors can have a pro-tumorigenic role, promote angiogenesis, assist immune evasion by the recruitment of immunosuspressive cells into the TME, support metastasis and induce inflammation in cancer regions [14][15]. CAFs induce tumor invasiveness by their ECM stiffening properties [16]. Cancer cells can recruit activated fibroblasts by the release of growth factors. Transforming Growth Factor-β (TGF-β) is the key growth factor most cancer cells depend on for fibroblast activation [7]. An overview of CAF origin, cytokine production and their role has been shown in figure 1.

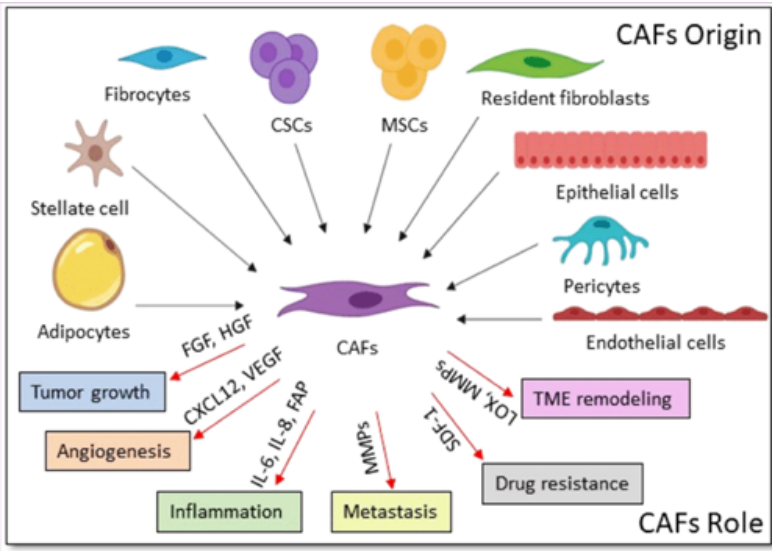

Figure 1: Origin and role of Cancer Associated Fibroblasts (CAFs) [17].

Pancreatic cancer is one of the most lethal cancers, with a 10-year survival rate of only 3%. Furthermore, pancreatic cancer accounted for 2.4% of new cases, and 6.5% of deaths caused by cancers in the Netherlands in 2019 [1]. Pancreatic Ductal Adenocarcinoma (PDAC) accounts for 90% of pancreatic cancers. Poor treatment outcomes are the result of late stage diagnosis, low probability of surgical operability and modest chemotherapy efficacy [18]. Though surgical resection clearly does increase survival rate, most diagnosed patients already have advanced stages of PDAC which makes resection impossible [18].

PDAC is characterized by increased fibrosis which results in a dense, stiff TME [19][20]. In fact, the PDAC TME has a tissue stiffness of around 10 kPa, while the Young's modulus of healthy pancreatic tissue lies around 0.5 kPa [20]. As previously mentioned, CAFs have a prominent function in the increased secretion of ECM components like Collagen I and Fibronectin. In PDAC, Pancreatic Stellate Cells (PSCs) are recruited and activated by cancer cells through TGF-β signalling to form much of the CAF population [7][21].

1.3 Mechanotransduction in cells

As briefly mentioned previously, cells receive many stimuli from their surrounding microenvironment, and neighboring cells. Next to for example growth factors and cytokines, cells also receive mechanical stimuli from the ECM. Mechanical cues like stiffness, shear stress and stretch are crucial for cells to adequately adapt to changes in their microenvironment and are involved with cell function regulation [22][23][24]. The process where cells sense, translate and react to mechanical signals is generally reverred to as mechanotransduction. Cells sense the ECM through Focal Adhesions (FAs). Focal Adhesions are complexes where the ECM, mainly fibronectin fibrils, and the cytoskeleton are connected through the trans-membrane heterodimeric integrin protein [10][25]. Focal Adhesions, and thus integrins, enable crosstalk of cells with their surrounding microenvironments [25]. Eighteen α- and eight β subunits combine to form one of 24 different integrin receptors [26]. Integrin protein can be bi-directionally activated. Extracellular integrin components generally have an intermediate affinity to bind ligands. When cells get activated by for example cytokines, intracellular processes stimulate integrin activation as talin binds to the intracellular β-tail of integrins [27]. This integrin activation increases integrin affinity to bind extracellular ligands, and is called 'inside-out' signalling. 'Outside-in' signalling, on the other hand, is induced by the extracellular integrin component inter-

acting with extracellular ligands, which enables cells to to sense their surrounding microenvironment and respond adequately. These bi-directional pathways often act simultaneously [27][28][29].

First identified in Drosophila, the Hippo signalling pathway is now known to have a key role in regulation cell proliferation and differentiation. Both biochemical and mechanical stimuli regulate the activation of Hippo signalling, which allows the Hippo pathway to have a pivotal role in cellular sensing [22][30]. Yes-Associated Protein (YAP) and Transcriptional Co-Activator with PDZ-Binding motif (TAZ) are the Hippo pathway effectors. These proteins are indispensable mechanotransducers in the Hippo pathway as they shuttle between the nucleus and cytoplasm to relay upstream mechanical (and biochemical) signals. By relaying signals to the nucleus, YAP/TAZ directly controls transcription of corresponding factors involved with cell proliferation and differentiation [24]. The Hippo signalling pathway can be active and inactive, depending on the received signals in cells. Growth inhibiting signals activates Hippo and causes YAP/TAZ to get phosphorylated. Phosphorylated YAP/TAZ is retained in the cytoplasma thus inactivated. Growth stimulating signals inactivate Hippo causing dephosphorylation and activation of YAP/TAZ, which allows nuclear accumulation of YAP/TAZ.

YAP/TAZ activation gets regulated by mechanical cues through the pathway shown in figure 2. As shown, RhoA stimulates actin cytoskeleton formation when sensing high ECM stiffness. The actin cytoskeleton and the tensile forces that it endures directly inactivate the Hippo pathway by inhibiting LATS1/2 activation, therefore allowing YAP/TAZ to move to the nucleus. Indirect inhibition of LATS1/2 is initiated by inhibiting RAP2 and MAP4K respectively. High ECM stiffness, no cell-cell contact and cell stretching generally cause YAP/TAZ activation and thus accumulation in the nucleus [22][24].

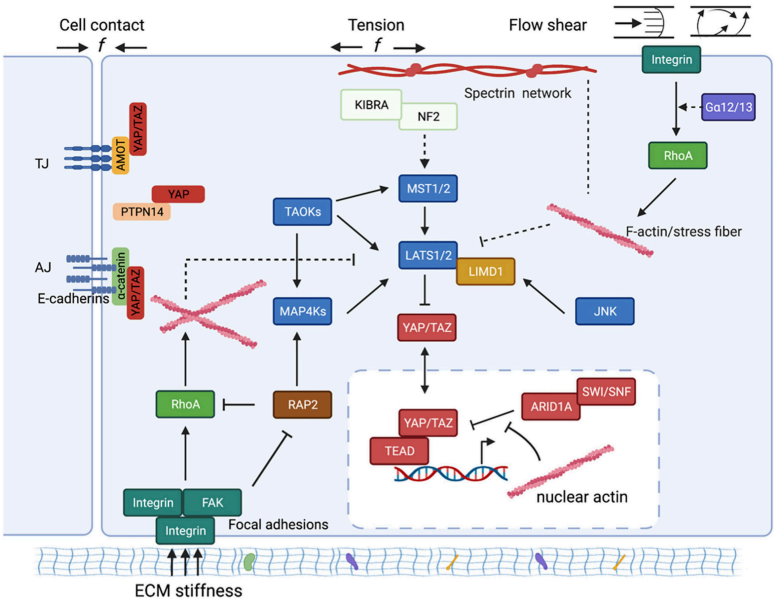

Figure 2: Schematic representation of mechanotransduction in the Hippo pathway. YAP/TAZ are the key effectors for mechanotransduction. High ECM stiffness, no cell-cell contact and cell stretching cause YAP/TAZ activation [22]

Integrins are an important contributor to mechanosensing. The $\alpha5\beta1$ integrin connects fibronectin to the cytoskeleton, after which mechanical stimuli can be transduced [10]. The $\alpha5\beta1$ integrins are an important group of integrins expressed by fibroblasts [28]. Furthermore, a previous study has found that CAFs mostly express $\alpha5\beta1$ integrins as well. Since CAFs have pro-tumorigenic roles in the TME, better knowledge about the potential of targeting $\alpha5\beta1$ integrins and inhibiting mechanosensing by these types of cells, could prove useful for future cancer therapeutics.

A recent study developed a novel therapeutic peptidomimetic, AV3, specifically against Integrin Subunit Alpha 5 (ITGA5). AV3 is the minimal sequence, consisting of seven amino acids, that is responsible for binding fibronectin to $\alpha5\beta1$. The study showed that AV3 is in fact binding specifically to the $\alpha5$ integrin subunit. Finally it was demonstrated that AV3 binding to the ITGA5A receptor has an inhibiting effect on TGF-β mediated pancreatic stellate cell (PSC) activation in vitro, and was able to decrease tumor volume in mice [31]. Since AV3 is being increasingly studied, the focus currently lies on the promising cyclic AV3.3 (CyAV3.3), the cyclic version of AV3.

The biochemical aspects of the TME and $\alpha5\beta1$ integrins, and their influence on cell behaviour, proliferation and potential metastasis have been widely investigated. However, much uncertainty still exists about the role of mechanical stiffness in these processes. Therefore, this research specifically questions the effect of mechanical stiffness in fibroblast activation. Additionally, this study aims to show the inhibiting capabilities of the novel CyAV3.3 peptide on fibroblast activation in different matrix stiffness conditions. Given that mechanical stiffness has a role in cell proliferation and differentiation [9][22], it is expected that fibroblasts activate more in higher matrix stiffness conditions compared to lower matrix stiffnesses. Secondly, since AV3 has been shown to inhibit PSC activation [31], it is expected that CyAV3.3 shows this inhibitory effect as well. Furthermore, as matrix stiffness is sensed through $\alpha5\beta1$ integrins, the inhibitory effect of CyAV3.3 is expected to be more prominent in high stiffness environments. The findings should generate new insight in ECM-PSC interactions. Improved understanding of these interactions can reflect on recruitment and activation of CAFs, which is relevant for improving cancer treatment efficacy.

2 Materials and methods

2.1 Materials

Collagen I was obtained from Matrix BioScience (GmbH, Mörlenbach, Germany). Human fibronectin was purchased from RD systems Inc. (Minneapolis, MN, USA). Bovine Serum Albumin (BSA) was acquired from VWR Life Science (Radnor, PA, USA). TGF-β was purchased from RD Systems Inc. (Minneapolis, MN, USA). Both AV3 and Cyclic AV3.3 (CyAV3.3) were obtained from China Peptide Co. Ltd. (Shanghai, China). The Cytosoft® 0.2 kPA (CC313)- and Cytosoft® 32 kPA (CC318) imaging 96-wells plate were purchased from Sigma-Aldrich (St. Louis, MO, USA). Mouse anti-YAP monoclonal IgG was purchased from Santa Cruz Biotechnology Inc. (Dallas, TX, USA). Mouse anti-αSMA monoclonal IgG (A2547) was purchased from Sigma-Aldrich (St. Louis, MO, USA). Goat anti-hITGA5 monoclonal IgG was obtained from RD Systems Inc. (Minneapolis, MN, USA). Mouse anti-YAP monoclonal IgG was obtained from Santa Cruz Biotechnology Inc. (Dallas, TX, USA). Donkey anti-mouse Alexa Fluor 488 was purchased from Thermo Fisher Scientific Inc. (Waltham, MA, USA). Goat anti-mouse Alexa Fluor 594 was purchased from Thermo Fisher Scientific Inc. (Waltham, MA, USA). Donkey anti-goat Alexa Fluor 488 was purchased from Thermo Fisher Scientific Inc. (Waltham, MA, USA). Fluoroshield^{tm} with DAPI was obtained from Merck KGaA (Darmstadt, Germany).

2.2 Study design

This study was designed to investigate mechanical stiffness as PSC activation mediator and to assess the inhibiting properties of the novel peptidomimetics (AV3 and CyAV3.3) on PSC activation. Since ITGA5 is a fibronectin receptor, we coated the wells with this ECM protein. Collagen I was taken as control. Immunofluorescence assays were used to investigate PSC activation. Immunofluorescent stainings were quantified and influence of mechanical stiffness and CyAV3.3 treatment were analysed.

The experiment was run twice with anti-YAP antibodies, twice with anti-ITGA5 antibodies and once with anti-αSMA antibodies.

2.3 Cells

Human pancreatic stellate cells (hPSCs) were purchased from ScienCell^{TM} (Carlsbad, CA, USA) and cultured with Stellate Cell Medium (SteCM) supplemented with 2% v/v Fetal Bovine Serum (FBS), 1% v/v Stellate cell growth supplement (SteCGS), and 1% v/v Penicillin-Streptomycin (Pen/Strep). Pancreatic Stellate Cells between passage 2 and 8 were used for the experiments.

2.4 PSC activation study

This experiment was conducted using three different well plates with a clear, rather extreme, low-high stiffness difference: Cytosoft® 0.2 kPA (CC313) imaging 96-wells plate, Cytosoft® 32 kPa (CC318) imaging 96-wells plate (Cytosoft®) and a normal non-tissue culture treated ELISA plastic 96-wells plate. The 0.2- and 32 kPa plates have been specifically

Prior to cell seeding, the plate was coated with 5 μg/cm^2 Fibronectin (RD Systems, Inc., Minneapolis, MN, USA) or 5 μg/cm^2 Collagen I (Matrix BioScience GmbH, Mörlenbach, Germany). Collagen I was taken as control. The coating concentrations are common for this application. 100μL of coating solution was added to the wells and incubated for 1 hour at room temperature, using a shaker at 150 RPM. Next, the shaker was turned off and the plate was incubated for an additional 2 hours at room temperature inside a Laminar Flow (LAF) cabinet. After incubation, unbound coating solution was removed from the wells. The experiment was also run once without coating the wells and once with a 5 μg/cm^2 Bovine Serum Albumin coating using the method mentioned above.

Human Pancreatic Stellate Cells (hPSCs) were seeded in a 96-well plate at a cell density of 5,000 cells/cm^2 and maintained in 2% FBS Stellate Cell Medium (SteCM). 24 hours after seeding, the cells were washed with DPBS once and starved in serum-free SteCM for another 24 hours. On the next day, the starvation medium was removed and the wells were treated. Cells were treated with 2% FBS SteCM which was supplemented with 5 ng/ml TGF-β (RD Systems, Inc., Minneapolis, MN, USA), 50 μM AV3 (China Peptide Co. Ltd. Shanghai, China) or 50 μM CyAV3.3 (China Peptide Co. Ltd. Shanghai, China; 99.06% purity) for the different conditions. These concentrations are common for this application.

The cells were incubated with the treatment solution for 24 hours instead of the more commonly practised 48 hours. This was done to decrease total incubation time, which is necessary since incubation time, if too long, can influence PSC activation. After these 24 hours of incubation, the wells were washed three times with DPBS and fixed with 4% formaldehyde for 15 minutes. Next, cells were permeabilized by treatment with 0.01% Triton X-100 in PBS solution for 5 minutes. Unspecific sites were blocked by adding a 0.05% Tween-20 in 2% BSA solution for 1 hour at room temperature, using a shaker at 150 RPM. Thereafter, the cells were incubated for 1 hour at room temperature with primary antibodies diluted in 0.05% Tween-20 in 2% BSA, using a shaker at 150 RPM. Used primary antibodies and recommended dilutions are summarized in table 1 in the appendices. Following the incubation with primary antibodies, the cells were washed five times with PBS and incubated for 1 hour at room temperature with the corresponding secondary antibodies diluted in 0.05% Tween-20 in 2% BSA, using a shaker at 150 RPM. Used secondary antibodies and recommended dilutions are summarized in table 1 in the appendices. The wells were washed five times with PBS and mounted in Fluoroshield^{TM} with DAPI (Merck KGaA, Darmstadt, Germany). Immunofluorescence staining was captured with the EVOS imaging system (Thermo Fisher Scientific Inc., Waltham, MA, USA).

Illumination settings were kept constant for all images. To account for variability within one well, three representative pictures were taken per well. Images were further processed- and quantified in Fiji ImageJ [32].

2.5 Fiji ImageJ quantification

Immunofluorescence stainings were quantified with the Fiji ImageJ software [32].

Acquired EVOS pictures were loaded into Fiji ImageJ, after which αSMA and ITGA5 intensities were quantified using the Threshold function. First, the Threshold was calibrated in such a way that the picture with the lowest intensity showed virtually negligible signal (αSMA = 50-255 ; ITGA5 = 30-255). Then, the area percentage of remaining signal within the calibrated Threshold was noted and normalized to the amount of cells visible in the picture. The resulting value was averaged over all pictures from the same condition. This process was repeated for all conditions.

YAP intensities were quantified using a different method. Since activated YAP shows nuclear localization instead of cytoplasmic, quantification focused on calculating the percentage of the total YAP/TAZ intensity that was localized in the nucleus. To achieve this, analyses were conducted using the Intensity Ratio Nuclei Cytoplasm Tool in Fiji ImageJ (Intensity Ratio Nuclei Cytoplasm Tool, RRID:SCR-018573). Pictures with saturated intensities were excluded (>0.500 area%)

2.6 Statistical analysis

Statistical analysis has been conducted to asses significant different between conditions. ANOVA one-way analyses of variance was used. Data was considered to be statistically significant at $p<0.05$ (*), $p<0.01$ (**).

3 Results

This study was designed to investigate mechanical stiffness as PSC activation mediator and to assess the inhibiting properties of the novel peptidomimetics (AV3 and cyclic AV3.3) on PSC activation.

The plastic well plate did not have a silicon coating to provide a specific matrix stiffness. As the two Cytosoft® plates do, the results of these different types of plates cannot be compared. Therefore, results retrieved from the plastic well plate are excluded from this section, and included in the appendices. Furthermore, cells seeded on uncoated and 2% BSA coated wells did not attach. These results have been excluded as well.

3.1 Mechanical stiffness in PSC activation

Immunofluorescence staining was used on PSCs to visualize αSMA-, ITGA5- and YAP expression in different matrix stiffness conditions. First, wells were coated with 5 μg/cm^2 fibronectin or 5 μg/cm^2 collagen I. Then, PSCs were seeded and starved with serum-free SteCM after 24 hours. Cells were treated with 5 ng/mL TGF-β in complete SteCM, or maintained with complete SteCM for an additional 24 hours. After the total 72 hours of incubation, cells were fixed and stained for αSMA-, ITGA5- and YAP. Fluoroshield^{TM} with DAPI was administered as final step of the process. αSMA-ITGA5 and YAP intensity levels for varying stiffness conditions were compared for PSCs seeded in fibronectin coated wells and treated with- and without TGF-β. Collagen I was taken as control.

First looking at cell morphology, we observe a combination of round- and elongated stretched cells for

both 32 kPa and 0.2 kPa conditions. Elongated cells seem to be less frequent for TGF-β treated PSCs.

As shown in figure 3A, a lower αSMA intensity was visible for non-treated PSCs in 0.2 kPa matrix stiffness conditions compared to non-treated PSCs in 32 kPa matrix stiffness conditions. The difference was statistically significant ($p<0.01$). Surprisingly, αSMA intensity was lower for TGF-β treated PSCs compared to non-treated PSCs in both matrix stiffness conditions. These observations were confirmed by quantifying αSMA expression intensities (figure 3B). For each condition 50 to 100 cells were analyzed (n=1).

Figure 3C presents ITGA5 intensity levels. No statistically significant differences were found comparing the 32 kPa- and 0.2 kPa matrix stiffness conditions. TGF-β treated PSCs showed an increase of ITGA5 intensity for both matrix stiffness conditions. The increase was statistically significant ($p<0.01$). Though, again no statistical significant difference was found comparing both matrix stiffness conditions. Quantification results, presented in figure 3D, confirmed these observations. In total, 80 to 180 cells were analyzed per condition (n=2).

As depicted in figure 3E-F, non-treated PSCs do not show a statistical significant difference in nuclear YAP percentage. Though, TGF-β treatment did reveal statistically significant difference of nuclear YAP/TAZ expression percentage for 32 kPa matrix stiffness compared to 0.2 kPa stiffness.

3.2 Novel peptidomimetic (AV3;CyAV3.3) in PSC activation

Immunofluorescence staining was used on PSCs to visualize αSMA-, ITGA5- and YAP intensity after treatment with the ITGA5 targeting peptide in different matrix stiffness conditions. First, wells were coated with 5 μg/cm^2 fibronectin or 5 μg/cm^2 collagen I. Then, PSCs were seeded and starved with serum-free SteCM after 24 hours. Cells were treated with complete SteCM which was supplemented with 5 ng/ml TGF-β, 50 μM AV3 or 50 μM CyAV3.3, or maintained with complete SteCM for an additional 24 hours. After the total 72 hours of incubation, cells were fixed and stained for αSMA-, ITGA5- and YAP. Fluoroshield^{TM} with DAPI was administered as final step of the process. αSMA-ITGA5 and YAP intensity levels for varying stiffness conditions were compared for PSCs seeded in fibronectin coated wells and treated with- and without TGF-β, CyAV3.3 and AV3. Collagen I was taken as control.

As depicted in figure 4A-B, αSMA intensity was decreased for PSCs in 32 kPa matrix stiffness conditions treated with CyAV3.3 and AV3. As shown in figure 5A, the difference was statistically significant for CyAV3.3 and AV3 ($p<0.05$ and $p<0.01$ respectively). In 0.2 kPa matrix stiffness conditions, no significant decrease of αSMA intensity was visible. In fact, compared to non-treated PSCs, αSMA expression seems to increase for AV3 treated PSCs. TGF-β treated PSCs also did not reveal significant decrease in αSMA expression intensity. Figure 4C-D display resulting ITGA5 expression intensity after treatment with the ITGA5 targeting peptides CyAV3.3 or AV3. Interestingly, ITGA5 expression of non-TGF-β treated cells seemed to increase as they were treated with CyAV3.3 or AV3. However, this trend was not visible for TGF-β treated PSCs. Here, expression intensity was lower when PSCs were treated with CyAV3.3 and lowest for AV3 treatment. The difference was confirmed to be statistically significant for TGF-β treated PSCs ($p<0.01$)(figure 5). As shown in figure 4E-F, nuclear YAP/TAZ accumulation did not visually show to be affected by peptide treatment. Though figure 5C showed significant decrease for CyAV3.3 treatment, and no decreased intensity for AV3 treated cells.

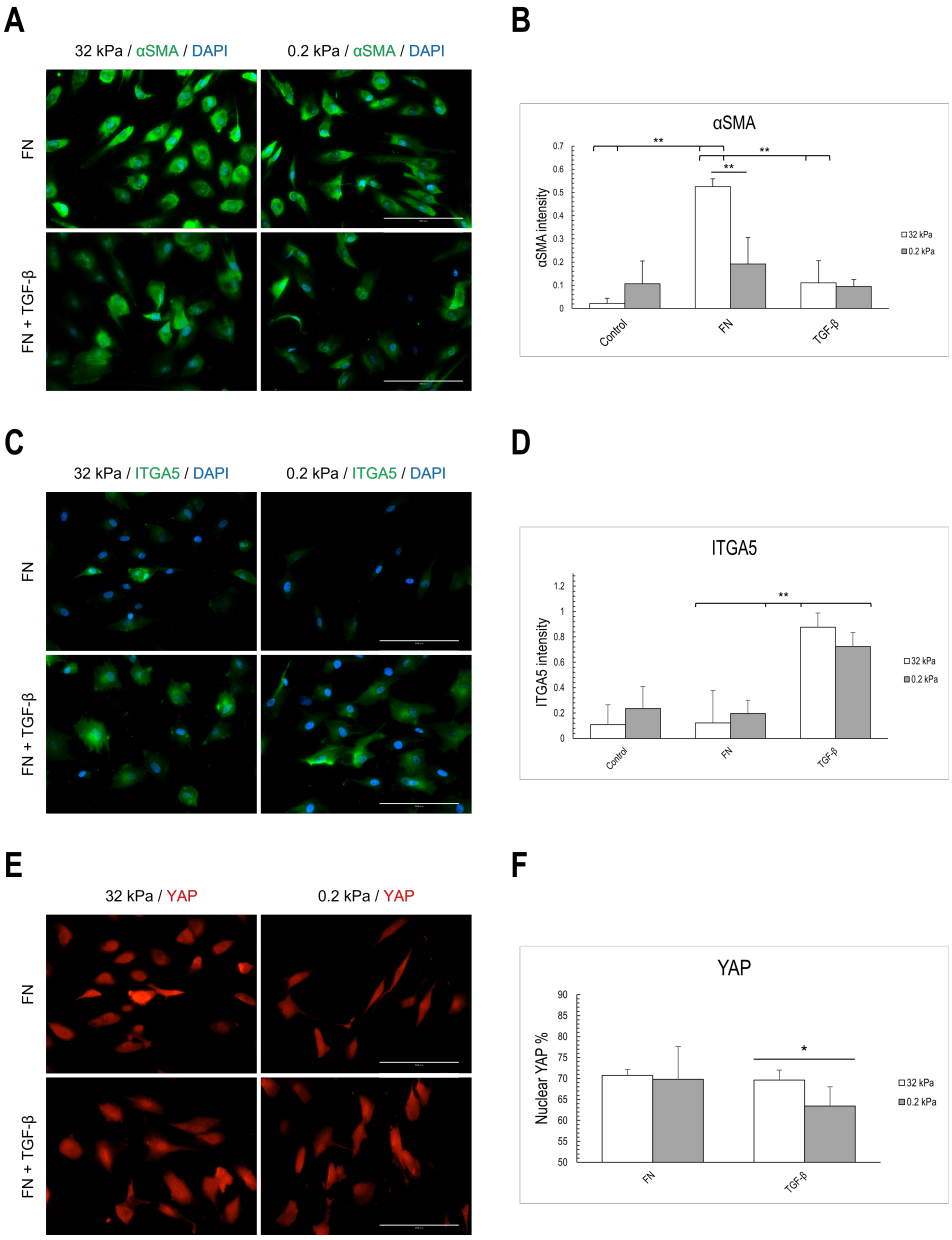

Figure 3: (A,C,E): Immunofluorescence staining of PSCs in 32 kPa and 0.2 kPa matrix stiffness conditions after 72h of culture. Magnification = 20x ; Scale bar = 200 μm. **(A):** Staining for mouse anti-αSMA monoclonal IgG (Green) and DAPI (Blue) showing αSMA intensity levels. αSMA intensity is lower for the 0.2 kPa matrix stiffness conditions. No increase in αSMA intensity was detected after TGF-β treatment (n=1). **(B):** Immunofluorescence αSMA expression intensity quantification with collagen I control. αSMA expression intensity normalized to number of cells. Statistical significant difference between non-TGF-β treated matrix stiffness conditions. Data represents means $\pm$ SD, $p<0.05$ (*), $p<0.01$ (**). **(C):** Staining for goat anti-ITGA5 monoclonal IgG (Green) and DAPI (Blue) showing ITGA5 intensity levels. No difference was found between both matrix stiffness conditions. TGF-β treated PSCs revealed an increase of ITGA5 expression intensity compared to non-treated PSCs (n=2). **(D):** Immunofluorescence ITGA5 expression intensity quantification with collagen I control. ITGA5 expression intensity normalized to number of cells. No statistical significant difference between matrix stiffness conditions. Statistical significant increase of ITGA5 intensity in TGF-β treated PSCs. Data represents means $\pm$ SD, $p<0.05$ (*), $p<0.01$ (**). **(E):** Immunofluorescence staining for mouse anti-YAP monoclonal IgG (Red) showing YAP expression intensity. No considerable difference found between matrix stiffness conditions. PSCs (n=2). **(F):** Immunofluorescence YAP expression intensity quantification. Nuclear YAP percentage differs significantly between matrix stiffness conditions for TGF-β treated PSCs. Data represents the mean nuclear YAP percentage $\pm$ SD, $p<0.05$ (*), $p<0.01$ (**).

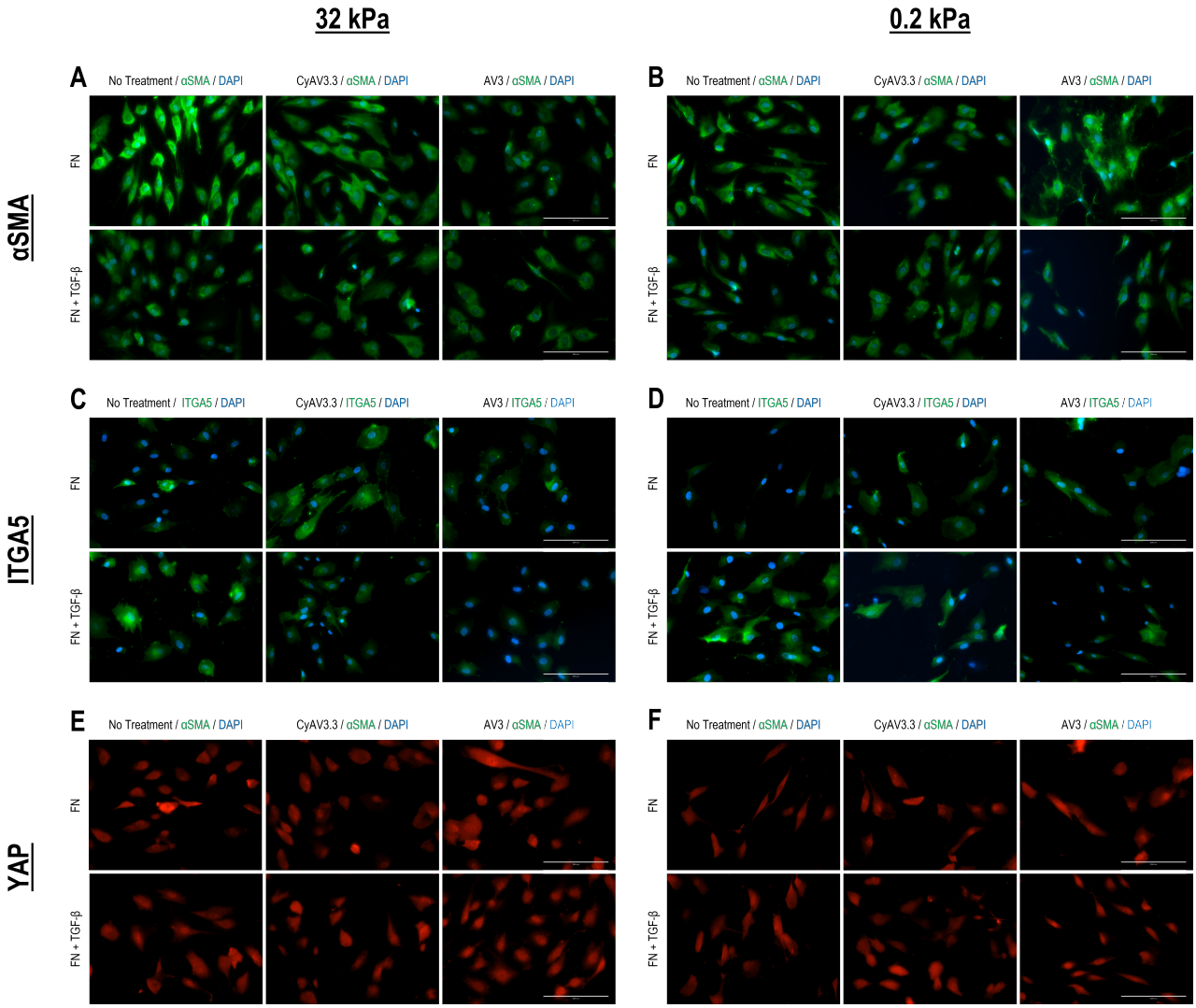

Figure 4: Immunofluorescence staining of PSCs with CyAV3.3/AV3 treatment in 32 kPa and 0.2 kPa matrix stiffness conditions after 72h of culture. Magnification = 20x ; Scale bar = 200 μm. **(A-B):** Staining for mouse anti-αSMA monoclonal IgG (Green) and DAPI (Blue) showing αSMA intensity levels. αSMA expression intensity of 32 kPa matrix stiffness conditions decreased after peptide treatment. No difference in αSMA intensity visible for TGF-β treated PSCs after treatment (n=1). **(C-D):** Staining for goat anti-ITGA5 monoclonal IgG (Green) and DAPI (Blue) showing ITGA5 intensity levels. Non TGF-β treated PSCs show higher ITGA5 intensities after peptide treatment. TGF-β treated PSCs reveal decreased ITGA5 expression intensity after peptide treatment (n=2). **(E-F):** Staining for mouse anti-YAP monoclonal IgG (RED) showing YAP/TAZ intensity levels. Nuclear YAP/TAZ expression seems similar in all conditions. 0.2 kPa seems to contain cells with smaller cell nucleï (n=2).

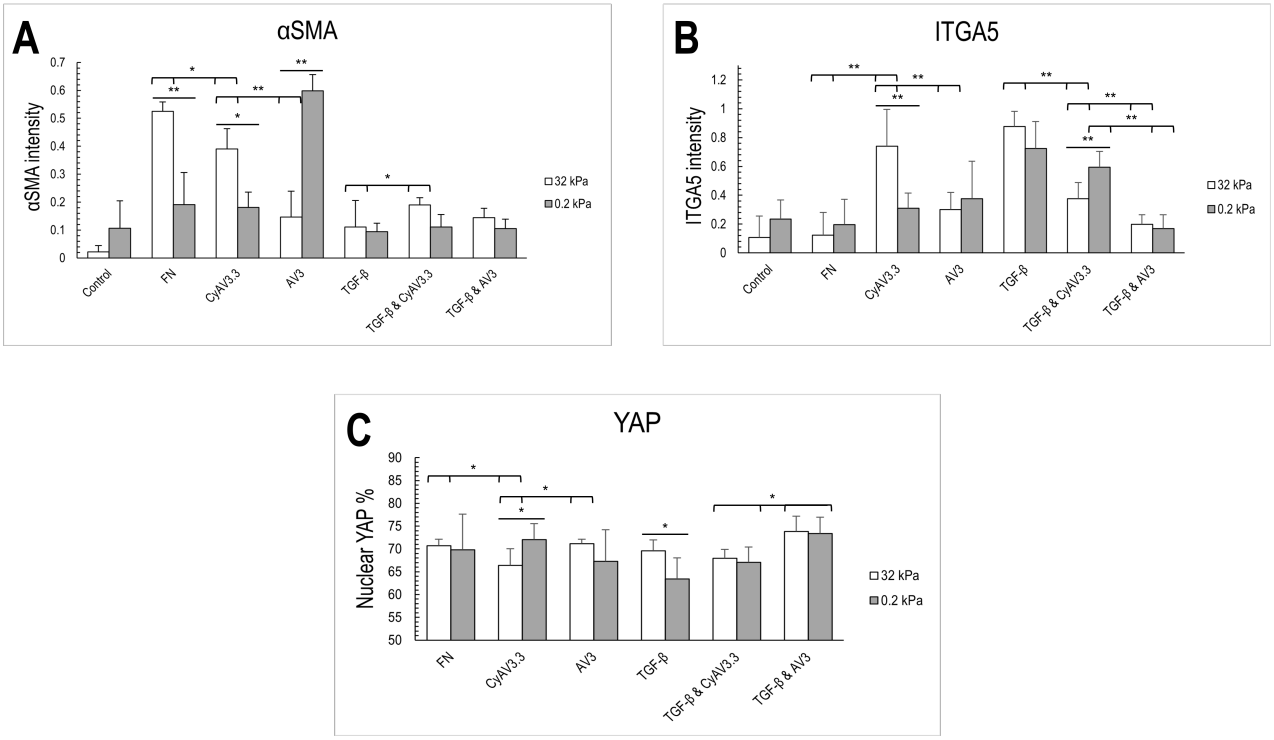

Figure 5: (A): Immunofluorescence αSMA intensity quantification with collagen I control. αSMA expression intensity normalized to number of cells. Statistical significant difference between non-TGF-β treated matrix stiffness conditions. Data represents means $\pm$ SD, $p<0.05$ (*), $p<0.01$ (**).**(B):** Immunofluorescence ITGA5 intensity quantification with collagen I control. ITGA5 expression intensity normalized to number of cells. Statistical significant difference between matrix stiffness conditions. Statistical significant increase of ITGA5 intensity in TGF-β treated PSCs. Data represents means $\pm$ SD, $p<0.05$ (*), $p<0.01$ (**). **(C): (F):** Immunofluorescence YAP intensity quantification. Intensity values are rather similar. CyAV3.3 did reveal significant decrease of YAP/TAZ expression intensity. Data represents the mean nuclear YAP percentage $\pm$ SD, $p<0.05$ (*), $p<0.01$ (**).

4 Discussion

Targeting the tumor microenvironment has been increasingly studied during the past years. It has become clear that the TME drastically influences the efficacy of therapeutic agents and can positively influence tumor growth. Cancer Associated Fibroblasts have been identified as major TME component and can have a pro-tumorigenic role. They play a vital role in tumor fibrosis and secrete growth factors and cytokines that support tumor growth. Inhibiting CAF activation and recruitment, and therefore reducing its pro-tumorigenic role, could prove valueable in cancer therapeutics. It has been well established that TGF-β can recruit and activate fibroblasts. Though, debate still continues about the exact role of mechanical stiffness in this process. Previous research has revealed that CAFs express high levels of $\alpha5\beta1$ integrins, which are essential for mechanosensing and -transduction. To inhibit this integrin, researchers have developed novel ITGA5 targeting peptides called AV3 and CyAV3.3, which are based on the same amino acid composition. In this study, we show indications that increasing matrix stiffness has a role in fibroblast activation. We corroborate ITGA5 up-regulation as a result of TGF-β treatment. Furthermore, we show decreasing fibroblast activation trends after treatment with the ITGA5 targeting peptides that could indicate inhibiting properties of CyAV3.3 and AV3. However, as explained below, these results should be interpreted with caution.

4.1 Mechanical stiffness influences PSC activation

αSMA immunofluorescence staining showed higher αSMA expression, and thus activation, on the 32 kPa matrix stiffness plate relative to the 0.2 kPa stiffness plate. The difference was statistically significant ($p<0.01$). However, ITGA5 expression did not show the same relation. The combination of these findings are counterintuative as they do not support previous research, which has found that ITGA5 expression decreased on lower matrix stiffness substrates [33]. Additionally, as mechanosensing by integrins influences cytoskeleton production, it was hypothesized that an increase in αSMA expression would be accompanied by increased ITGA5 expression. The difference in PSC activation as a result of matrix stiffness, indicated by the increased αSMA expression, is not evident from our mechanotransduction effector YAP/TAZ results either. An increase of stiffness mediated activation would suggest an increase in nuclear YAP/TAZ localization, which is not the case.

A possible explanation for this result might be that the nuclear YAP/TAZ was saturated. A recent study found that nuclear YAP/TAZ expression levels in mesenchymal stem cells (MSCs) plateaued after 10 kPa matrix stiffness, at which the researchers found nuclear YAP/TAZ percentages between 70%-90% [34]. The border limit of these nuclear expression levels are comparable to our data. Although the particular study did not include PSCs, there are similarities between both types of cells. Since MSCs also get recruited in pancreatic cancers and are part of the CAF population, it can be suggested that YAP/TAZ mechanisms and -saturation levels are similar [35]. Yet, if 32 kPa matrix stiffness would in fact saturate nuclear YAP/TAZ, it does not explain why 0.2 kPa shows similar levels of nuclear YAP/TAZ. This discrepancy could be attributed to the fact that stiffness is not the sole factor that influences the activity of the hippo pathway. As previously mentioned, factors like cell stretching can also induce YAP/TAZ activation [22][23][24]. As mentioned in the results section, the reviewed pictures showed cells with similar cell stretching. This observation could explain similar YAP/TAZ activation levels. To test this hypothesis, pictures from this study can be further analyzed in the future using image process software like ImageJ, to quantify cell stretching in these conditions.

As discussed, ITGA5 expression did not show stiffness mediated differences either. It is difficult to explain this result, but closer inspection to the standard deviations presented in figure 3D reveal broad variation within the analysed population. This could indicate that the analysed pictures do not adequately represent the population.

Although the observed αSMA expression, and thus activation, is consistent with suggestions made in literature [9][23], another possible explanation for the contradictions between αSMA, ITGA5 and YAP/TAZ has to do with the fact that the αSMA immunofluorescence staining experiment was only run once. Therefore, it is cannot be ruled out that the increased αSMA expression for the high stiffness condition could be a false positive. Running additional experiments to investigate αSMA expression might be valuable to include in future research.

Conditions were also studied with TGF-β treatment, that has been shown to activate fibroblasts [7]. Since TGF-β treated cells consistently expressed lower αSMA levels, this study has been unable to demonstrate TGF-β mediated PSC activation. A possible explanation is the fact that PSCs were incubated with the TGF-β treatment solution for just 24 hours, while 48 hours in commonly used. However, the choice to reduce treatment time, and thus total incubation time, was well considered. As stated, the aim of this study is to capture the influence of mechanical stiffness in fibroblast activation. Knowing that cells will activate after a yet undefined period of incubation regardless of matrix stiffness, it was crucial to keep total incubation time relatively short.
Meanwhile, ITGA5 expression increased significantly after TGF-β treatment. This is consistent with other previous studies that demonstrated TGF-β activates and up-regulates ITGA5 expression [31][36].

Nuclear expression of YAP/TAZ did not increase after TGF-β treatment. Although crosstalk between the Hippo- and TGF-β pathway had been previously suggested [37], these results do not show a correlation.

4.2 Novel ITGA5 targeting peptides CyAV3.3 and AV3 inhibit PSC activation

Treatment with the novel ITGA5 targeting peptides CyAV3.3 and its predecessor AV3 showed significant decrease in αSMA expression for 32 kPa matrix stiffness. 0.2 kPa matrix stiffness did not reveal a significant decrease. One unanticipated finding was the sudden increase of AV3 treated PSCs in the 0.2 kPa conditions. This result could be explained by the fact that CyAV3.3 and AV3 target the ITGA5 receptor, which is involved with mechanosensing. When ITGA5 binds the peptide, cells would theoretically have decreased sense of matrix stiffness, which would decrease matrix stiffness mediated activation. This hypothesis is supported by the observations. The sudden increase of αSMA expression after AV3 treatment is not expected to be representative. Since the results contradict expectations and show much higher αSMA expression compared to the untreated PSCs, it is believed to be an outcast. As mentioned, αSMA results rely on one experiment, which makes it difficult to prove this explanation. Therefore, future research could focus on repeating the experiment to validate whether or not these results are representative.

ITGA5 expression after treatment did not show stiffness induced differences. No decrease of ITGA5 expression was found for non-TGF-β treated cells. Although ITGA5 expression increased after CyAV3.3 treatment, AV3 treated cells showed a significant decrease relative to CyAV3.3. Comparing ITGA5 expression levels for CyAV3.3 and decreased levels and AV3, we recognize a trend similar to the αSMA results. Assuming this trend is valid, it supports the previously mentioned indications that non-treated PSC ITGA5 data might not be representative.

Nuclear YAP/TAZ expression levels did significantly decrease after CyAV3.3 treatment. Though result are contradicting since AV3 does not seem to have an effect. Uniformity between αSMA, ITGA5 and YAP/TAZ expression was expected because mechanosensing by integrins, mechanotransduction through YAP/TAZ and activation of fibroblasts are connected [22]. This result might be explained by a delay in YAP/TAZ inactivation. αSMA expression is regulated by RhoA (Rho family) [12]. Closer inspection of the Hippo pathway shows that RhoA is upstream of YAP/TAZ [22], which suggests ITGA5 and RhoA activity will respond first to inhibition by CyAV3.3 and AV3. Since ITGA5- and αSMA results implicate inhibition by both peptides, and YAP/TAZ is located downstream in the mechanotransduction pathway, we can infer that YAP/TAZ inhibition might be delayed. Future work might investigate the likelyhood of YAP/TAZ inhibition delay by increasing treatment time from 24 hours to 48 hours.

Inhibiting properties of CyAV3.3 and AV3 have also been investigated in TGF-β mediated PSC activation. As previously stated, αSMA results unfortunately showed no TGF-β mediated activation. Therefore, this study was unable to investigate the inhibiting effect of CyAV3.3 and AV3 by evaluating αSMA expression after treatment with the peptides. Though, consistent with the literature [31], ITGA5 results showed that ITGA5 expression could be inhibited with CyAV3.3 and AV3 in TGF-β mediated PSC activation. Nuclear YAP/TAZ expression did not show uniform inhibition as a result of treatment with the novel peptides. Previously proposed explanations (saturation and inhibition delay) apply for TGF-β mediated activation as well.

4.3 Study limitations

This study contained several weaknesses that limit the generalisability and exposed the results to unknown variables that weaken its implications. First, the result showed lack of uniformity with literature as αSMA results showed that TGF-β did not seem to activate PSCs. Next, ITGA5 expression results did not suggest influence of matrix stiffness. Finally, nuclear YAP/TAZ expression generally showed constant expression for all conditions. There are some statistically significant relations, but these contradict each other. Consequently, results should be evaluated with caution.

A second weakness in this study, which could very much have affected PSC activation, is the fact that PSCs were treated with 2% FBS SteCM instead of serum-free SteCM. Using serum-free SteCM is the conventional method for drug treatment solutions. Since FBS contains various growth factors (e.g. TGF-β) itself, it can have a supporting role in PSC activation. Fortunately, the used medium contained 2% FBS, which comes down to 0.2-0.4 ng/mL latent TGF-β [38]. This study used TGF-β treatment concentrations of 5 ng/mL TGF-β, which is a ten fold higher. Therefore, the implications made in this study can still be considered for future research.

Furthermore, it is unfortunate that the study did not include fitting negative controls. First of all, the secondary antibodies could have been tested on unspecific binding by not adding a primary antibody. This could improved reliability of intensity quantifications and observations, which could further support the implications made in this study. Secondly, it was attempted to include a control for non-activated PSCs by seeding cells in uncoated- and 5 μg/cm^2 BSA coated wells. However, PSCs did not attach during both experiments. Further work might include a control where cells are cultured in serum-free medium during the whole experiment. Next to that, other types of coatings can be applied to enhance cell attachment. For example, Poly-L-Lysine can be used to enhance cell attachment by electrostatic interaction between negatively charged ions of the cell membrane and the culture surface.

A potential limitation of the study is that cells were not counted after the immunofluorescence staining. This might have been relevant since CyAV3.3 and AV3 target the ITGA5 fibronectin receptor. As integrins bind cells to the ECM, targeting such proteins could result in lower cell attachment. As mentioned in the result section, blank wells did not show cell attachment. Therefore, there is a possibility that cells which got heavily targeted by CyAV3.3- and AV3 detached during washing steps. This would mean that cells showing the inhibiting effect might have been unintentionally removed. Fortunately, such occurrence would only make the actual findings of this study increasingly significant. Though, this study would have been more useful if cell count was included.

4.4 Recommendations

As mentioned in the previous sections, this work needs additional experiments to validate and strengthen our findings. The experiment could be rerun with αSMA and ITGA5 immunofluorescence staining to investigate if the interpreted results in this study are valid. Furthermore, treatment time could be increased back to 48 hours to investigate the low αSMA expression this study observed after TGF-β treatment. Including treatment with CyAV3.3 and AV3 would enable future researchers to investigate if the found YAP/TAZ results are in fact caused by a delay in response to the inhibiting effects of the novel peptides. Further analysis of our pictures (e.g. stretch assay) could be valuable to investigate mechanisms that could contribute to PSC activation, and YAP/TAZ activation. Although our findings did not express its immediate necessity, running a control experiment to asses the influence the 2% FBS present in our treatment medium could be valuable.

In addition to the recommended work to validate the implications made in this study, future studies can also focus on acquiring more knowledge about influence of matrix stiffness and the effect of the novel peptides. Cell attachment assays under treatment of CyAV3.3 can be done to assess the degree to which the novel peptide interacts with already attached cells. Cell attachment without CyAV3.3 treatment would be compared with attachment with treatment. In addition, the moment of treatment relative to moment of cell seeding can be varied as well. Cell attachment without treatment would be included as positive control. Treatment with Bovine Serum Albumin could be included as negative control, as BSA has been found to prevent cell attachment [39]. Next CyAV3.3 can be added after 48 hours culture (including cell starvation), and simultaneously to cell seeding. Results could suggest an optimal focus of CyAV3.3 in therapeutic applications: prevent, or inhibit PSC activation.

If the results from this study have been validated by future research and confirm our findings, an overarching study could be considered. A further study could assess directly how tumor cell viability is affected by fibroblasts cultured on different matrix stiffness conditions. This could be achieved by treating tumor cells with 0% FBS medium which is supplemented with a maximum of 50% condition medium from cultured fibroblasts. Thus, such a study would investigate if fibroblasts secrete increased amounts of tumor promoting factors in stiff matrix environments relative to soft matrix environments. Treating fibroblasts with CyAV3.3 and studying its eventual results on tumor cell viability could also be included.

5 Conclusion

This study investigated the effect of mechanical stiffness in fibroblast activation. Additionally, this study aimed to show the inhibiting capabilities of the novel CyAV3.3 peptide on fibroblast activation in different matrix stiffness conditions. To examine these questions, αSMA, ITGA5 and YAP/TAZ expression levels were visualized by immunofluorescence staining. It was hypothesized that increased matrix stiffness would induce upregulation of these proteins. CyAV3.3 treatment was expected to show downregulation in the same proteins. Furthermore, CyAV3.3 inhibition was expected to be more significant in high matrix stiffness environments.

The study found upregulated αSMA expression for high matrix stiffness. CyAV3.3 showed significant downregulation of αSMA in high matrix stiffness conditions for non-TGF-β treated PSCs. The inhibiting effect of CyAV3.3 was also seen for ITGA5 in TGF-β mediated PSC activation. These findings only partially confirm the hypothesis, as YAP/TAZ activation did not show uniform and significant change for both mechanical stiffness and CyAV3.3. Future research is required to validate our αSMA and ITGA5 findings. Further, cell attachment experiments under treatment of CyAV3.3 could shed more light on the efficacy of CyAV3.3 in different ITGA5 stages.

In spite of its limitations, the study adds to the understanding of the role of mechanical stiffness in PSC activation. Furthermore, we provide supporting data that indicates the inhibiting effect of CyAV3.3 on PSC activation, which is relevant for improving cancer treatment efficacy.

6 Acknowledgements

First of all, I would like to thank Prof. Dr. Jai Prakash for giving me the opportunity to work on such an interesting assignment. I received much support from him during my relatively short time at the Advanced Organ Bioengineering and Therapeutics group. I would like to thank my daily supervisor Kunal Pednekar, MSc for assisting me in the lab, teaching me new techniques and giving feedback when needed. I would like to thank Dr. Janneke Alers for being the external member to my bachelor assignment committee, and evaluating my work. Finally, I would like to thank the whole AOT group for the welcoming atmosphere and the great times during the past 11 weeks.

References

[1] Netherlands Comprehensive Cancer Organisation (IKNL). *Cancer statistics*. 2021. URL: https://iknl.nl/en/ncr/ncr-data-figures (visited on 06/20/2022).

[2] Sara Charmsaz, Denis M. Collins, Antoinette S. Perry, et al. "Novel Strategies for Cancer Treatment: Highlights from the 55th IACR Annual Conference". In: *Cancers* 11.8 (Aug. 2019). ISSN: 20726694. DOI: 10.3390/CANCERS11081125. URL: /pmc/articles/PMC6721818/%20/pmc/articles/PMC6721818/?report=abstract%20https://www.ncbi.nlm.nih.gov/pmc/articles/PMC6721818/.

[3] Amber E. De Groot, Sounak Roy, Joel S. Brown, et al. "Revisiting Seed and Soil: Examining the Primary Tumor and Cancer Cell Foraging in Metastasis". In: *Molecular cancer research : MCR* 15.4 (Apr. 2017), p. 361. ISSN: 15573125. DOI: 10.1158/1541-7786.MCR-16-0436. URL: /pmc/articles/PMC5380470/%20/pmc/articles/PMC5380470/?report=abstract%20https://www.ncbi.nlm.nih.gov/pmc/articles/PMC5380470/.

[4] Erik Henke, Rajender Nandigama, and Süleyman Ergün. "Extracellular Matrix in the Tumor Microenvironment and Its Impact on Cancer Therapy". In: *Frontiers in Molecular Biosciences* 6 (Jan. 2020), p. 160. ISSN: 2296889X. DOI: 10.3389/FMOLB.2019.00160/BIBTEX.

[5] Utpreksha Vaish, Tejeshwar Jain, Abhi C. Are, et al. "Cancer-Associated Fibroblasts in Pancreatic Ductal Adenocarcinoma: An Update on Heterogeneity and Therapeutic Targeting". In: *International Journal of Molecular Sciences* 22.24 (Dec. 2021). ISSN: 14220067. DOI: 10.3390/IJMS222413408. URL: /pmc/articles/PMC8706283/%20/pmc/articles/PMC8706283/?report=abstract%20https://www.ncbi.nlm.nih.gov/pmc/articles/PMC8706283/.

[6] Valerie S. LeBleu and Raghu Kalluri. "A peek into cancer-associated fibroblasts: origins, functions and translational impact". In: *Disease Models & Mechanisms* 11.4 (Apr. 2018). ISSN: 17548411. DOI: 10.1242/DMM.029447. URL: /pmc/articles/PMC5963854/%20/pmc/articles/PMC5963854/?report=abstract%20https://www.ncbi.nlm.nih.gov/pmc/articles/PMC5963854/.

[7] Raghu Kalluri. "The biology and function of fibroblasts in cancer". In: *Nature Reviews Cancer 2016 16:9* 16.9 (Aug. 2016), pp. 582–598. ISSN: 1474-1768. DOI: 10.1038/nrc.2016.73. URL: https://www.nature.com/articles/nrc.2016.73.

[8] E. Aikawa. "Immunohistochemistry". In: *Comprehensive Biomaterials* 3 (Oct. 2011), pp. 277–290. DOI: 10.1016/B978-0-08-055294-1.00100-8.

[9] Mirko D'Urso and Nicholas A. Kurniawan. "Mechanical and Physical Regulation of FibroblastMyofibroblast Transition: From Cellular Mechanoresponse to Tissue Pathology". In: *Frontiers in Bioengineering and Biotechnology* 8 (Dec. 2020), p. 1459. ISSN: 22964185. DOI: 10.3389/FBIOE.2020.609653/BIBTEX.

[10] Nikolaos G. Frangogiannis. "FibroblastExtracellular Matrix Interactions in Tissue Fibrosis". In: *Current pathobiology reports* 4.1 (Mar. 2016), p. 11. ISSN: 2167485X. DOI: 10.1007/S40139-016-0099-1. URL: /pmc/articles/PMC4860262/%20/pmc/articles/PMC4860262/?report=abstract%20https://www.ncbi.nlm.nih.gov/pmc/articles/PMC4860262/.

[11] Boris Hinz. "Myofibroblasts". In: *Experimental Eye Research* 142 (Jan. 2016), pp. 56–70. ISSN: 0014-4835. DOI: 10.1016/J.EXER.2015.07.009.

[12] Jiaxu Wang, Ron Zohar, and Christopher A. McCulloch. "Multiple roles ofăα-smooth muscle actin in mechanotransduction". In: *Experimental Cell Research* 312.3 (Feb. 2006), pp. 205–214. ISSN: 0014-4827. DOI: 10.1016/J.YEXCR.2005.11.004.

[13] James J. Tomasek, Giulio Gabbiani, Boris Hinz, et al. "Myofibroblasts and mechano-regulation of connective tissue remodelling". In: *Nature Reviews Molecular Cell Biology 2002 3:5* 3.5 (2002), pp. 349–363. ISSN: 1471-0080. DOI: 10.1038/nrm809. URL: https://www.nature.com/articles/nrm809.

[14] Fei Xing, Jamila Saidou, and Kounosuke Watabe. "Cancer associated fibroblasts (CAFs) in tumor microenvironment". In: *Frontiers in bioscience : a journal and virtual library* 15.1 (Jan. 2010), p. 166. ISSN: 27686698. DOI: 10.2741/3613. URL: /pmc/articles/PMC2905156/%20/pmc/articles/PMC2905156/?report=abstract%20https://www.ncbi.nlm.nih.gov/pmc/articles/PMC2905156/.

[15] Tongyan Liu, Chencheng Han, Siwei Wang, et al. "Cancer-associated fibroblasts: An emerging target of anticancer immunotherapy". In: *Journal of Hematology and Oncology* 12.1 (Aug. 2019), pp. 1–15. ISSN: 17568722. DOI: 10.1186/S13045-019-0770-1/TABLES/2. URL: https://jhoonline.biomedcentral.com/articles/10.1186/s13045-019-0770-1.

[16] Chang Liu and Michael Mak. "Fibroblast-mediated uncaging of cancer cells and dynamic evolution of the physical microenvironment". In: *Scientific Reports 2022 12:1* 12.1 (Jan. 2022), pp. 1–11. ISSN: 2045-2322. DOI: 10.1038/s41598-021-03134-w. URL: https://www.nature.com/articles/s41598-021-03134-w.

[17] Amira Osman, Said M. Afify, Ghmkin Hassan, et al. "Revisiting cancer stem cells as the origin of cancer-associated cells in the tumor microenvironment: A hypothetical view from the potential of iPSCs". In: *Cancers* 12.4 (Apr. 2020). ISSN: 20726694. DOI: 10.3390/CANCERS12040879.

[18] Daniel R. Principe, Patrick W. Underwood, Murray Korc, et al. "The Current Treatment Paradigm for Pancreatic Ductal Adenocarcinoma and Barriers to Therapeutic Efficacy". In: *Frontiers in Oncology* 11 (July 2021), p. 2773. ISSN: 2234943X. DOI: 10.3389/FONC.2021.688377/BIBTEX.

[19] Sujata Kane, PA-C, Anne Engelhart, ANP-BC, Jessica Guadagno, PA-C, et al. "Pancreatic Ductal Adenocarcinoma: Characteristics of Tumor Microenvironment and Barriers to Treatment". In: *Journal of the Advanced Practitioner in Oncology* 11.7 (Sept. 2020), p. 693. ISSN: 21500878. DOI: 10.6004/JADPRO.2020.11.7.4. URL: /pmc/articles/PMC7646635/%20/pmc/articles/PMC7646635/?report=abstract%20https://www.ncbi.nlm.nih.gov/pmc/articles/PMC7646635/.

[20] Benjamin M. Maccurtain, Ned P. Quirke, Stephen D. Thorpe, et al. "Pancreatic Ductal Adenocarcinoma: Relating Biomechanics and Prognosis". In: *Journal of clinical medicine* 10.12 (June 2021). ISSN: 2077-0383. DOI: 10.3390/JCM10122711. URL: https://pubmed.ncbi.nlm.nih.gov/34205335/.

[21] M V Apte, S Park, P A Phillips, et al. "Desmoplastic reaction in pancreatic cancer: role of pancreatic stellate cells." eng. In: *Pancreas* 29.3 (Oct. 2004), pp. 179–187. ISSN: 1536-4828 (Electronic). DOI: 10.1097/00006676-200410000-00002.

[22] Xiaomin Cai, Kuei Chun Wang, and Zhipeng Meng. "Mechanoregulation of YAP and TAZ in Cellular Homeostasis and Disease Progression". In: *Frontiers in Cell and Developmental Biology* 9 (May 2021), p. 1333. ISSN: 2296634X. DOI: 10.3389/FCELL.2021.673599/BIBTEX.

[23] Fabiana Martino, Ana R. Perestrelo, Vladimír Vinarský, et al. "Cellular mechanotransduction: From tension to function". In: *Frontiers in Physiology* 9.JUL (July 2018), p. 824. ISSN: 1664042X. DOI: 10.3389/FPHYS.2018.00824/BIBTEX.

[24] Sirio Dupont, Leonardo Morsut, Mariaceleste Aragona, et al. "Role of YAP/TAZ in mechanotransduction". In: *Nature* (2011). DOI: 10.1038/nature10137.

[25] Florence Schaffner, Anne Marie Ray, and Monique Dontenwill. "Integrin $\alpha5\beta1$, the Fibronectin Receptor, as a Pertinent Therapeutic Target in Solid Tumors". In: *Cancers* 5.1 (Mar. 2013), p. 27. ISSN: 20726694. DOI: 10.3390/CANCERS5010027. URL: /pmc/articles/PMC3730317/%20/pmc/articles/PMC3730317/?report=abstract%20https://www.ncbi.nlm.nih.gov/pmc/articles/PMC3730317/.

[26] Jonas Schnittert, Ruchi Bansal, Gert Storm, et al. "Integrins in wound healing, fibrosis and tumor stroma: High potential targets for therapeutics and drug delivery". In: *Advanced Drug Delivery Reviews* 129 (Apr. 2018), pp. 37–53. ISSN: 0169-409X. DOI: 10.1016/J.ADDR.2018.01.020.

[27] Jia Huai Wang. "Pull and push: Talin activation for integrin signaling". In: *Cell Research 2012 22:11* 22.11 (July 2012), pp. 1512–1514. ISSN: 1748-7838. DOI: 10.1038/cr.2012.103. URL: https://www.nature.com/articles/cr2012103.

[28] Sjoerd Van Helvert, Cornelis Storm, and Peter Friedl. "Mechanoreciprocity in cell migration". In: *Nature Cell Biology 2017 20:1* 20.1 (Dec. 2017), pp. 8–20. ISSN: 1476-4679. DOI: 10.1038/s41556-017-0012-0. URL: https://www.nature.com/articles/s41556-017-0012-0.

[29] Bo Shen, M Keegan Delaney, and Xiaoping Du. "Inside-out, outside-in, and inside-outside-in: G protein signaling in integrin-mediated cell adhesion, spreading, and retraction." eng. In: *Current opinion in cell biology* 24.5 (Oct. 2012), pp. 600–606. ISSN: 1879-0410 (Electronic). DOI: 10.1016/j.ceb.2012.08.011.

[30] Jyoti R Misra and Kenneth D Irvine. "The Hippo Signaling Network and Its Biological Functions." eng. In: *Annual review of genetics* 52 (Nov. 2018), pp. 65–87. ISSN: 1545-2948 (Electronic). DOI: 10.1146/annurev-genet-120417-031621.

[31] Praneeth R. Kuninty, Ruchi Bansal, Susanna W.L. De Geus, et al. "ITGA5 inhibition in pancreatic stellate cells attenuates desmoplasia and potentiates efficacy of chemotherapy in pancreatic cancer". In: *Science Advances* 5.9 (Sept. 2019). ISSN: 23752548. DOI: 10.1126/SCIADV.AAX2770. URL: /pmc/articles/PMC6726450/%20/pmc/articles/PMC6726450/?report=abstract%20https://www.ncbi.nlm.nih.gov/pmc/articles/PMC6726450/.

[32] Johannes Schindelin, Ignacio Arganda-Carreras, Erwin Frise, et al. "Fiji: an open-source platform for biological-image analysis". In: *Nature Methods 2012 9:7* 9.7 (June 2012), pp. 676–682. ISSN: 1548-7105. DOI: 10.1038/nmeth.2019. URL: https://www.nature.com/articles/nmeth.2019.

[33] Brijesh Kumar Verma, Aritra Chatterjee, Paturu Kondaiah, et al. "Substrate stiffness modulates integrin $\alpha5$ expression and ECM-associated gene expression in fibroblasts". In: *bioRxiv* (Nov. 2021), p. 2021.11.22.469526. DOI: 10.1101/2021.11.22.469526. URL: https://www.biorxiv.org/content/10.1101/2021.11.22.469526v1%20https://www.biorxiv.org/content/10.1101/2021.11.22.469526v1.abstract.

[34] Masashi YAMAZAKI, Satoru KIDOAKI, Hiromichi FUJIE, et al. "Designing Elastic Modulus of Cell Culture Substrate to Regulate YAP and RUNX2 Localization for Controlling Differentiation of Human Mesenchymal Stem Cells". In: *Analytical sciences : the international journal of the Japan Society for Analytical Chemistry* 37.3 (2021), pp. 447–453. ISSN: 1348-2246. DOI: 10.2116/ANALSCI.20SCP02. URL: https://pubmed.ncbi.nlm.nih.gov/33692265/.

[35] Yoshiaki Sunami, Johanna HäuSSler, and Jörg Klee. "Cellular Heterogeneity of Pancreatic Stellate Cells, Mesenchymal Stem Cells, and Cancer-Associated Fibroblasts in Pancreatic Cancer". In: *Cancers* 12.12 (Dec. 2020), pp. 1–15. ISSN: 20726694. DOI: 10.3390/CANCERS12123770. URL: /pmc/articles/PMC7765115/%20/pmc/articles/PMC7765115/?report=abstract%20https://www.ncbi.nlm.nih.gov/pmc/articles/PMC7765115/.

[36] Fahmy A. Mamuya and Melinda K. Duncan. "aV integrins and TGF-β-induced EMT: a circle of regulation". In: *Journal of Cellular and Molecular Medicine* 16.3 (2012), p. 445. ISSN: 15821838. DOI: 10.1111/J.1582-4934.2011.01419.X. URL: /pmc/articles/PMC3290750/%20/pmc/articles/PMC3290750/?report=abstract%20https://www.ncbi.nlm.nih.gov/pmc/articles/PMC3290750/.

[37] Liliana Attisano and Jeffrey L. Wrana. "Signal integration in TGF-β, WNT, and Hippo pathways". In: *F1000Prime Reports* 5 (June 2013). ISSN: 20517599. DOI: 10.12703/P5-17. URL: /pmc/articles/PMC3672943/%20/pmc/articles/PMC3672943/?report=abstract%20https://www.ncbi.nlm.nih.gov/pmc/articles/PMC3672943/.

[38] Takatoku Oida and Howard L. Weiner. "Depletion of TGF-β from fetal bovine serum". In: *Journal of immunological methods* 362.1-2 (Oct. 2010), p. 195. ISSN: 00221759. DOI: 10.1016/J.JIM.2010.09.008. URL: /pmc/articles/PMC2989462/%20/pmc/articles/PMC2989462/?report=abstract%20https://www.ncbi.nlm.nih.gov/pmc/articles/PMC2989462/.

[39] Frederick Grinnell and Marian K. Feld. "Initial adhesion of human fibroblasts in serum-free medium: Possible role of secreted fibronectin". In: *Cell* 17 (1 1979), pp. 117–129. ISSN: 00928674. DOI: 10.1016/0092-8674(79)90300-3.

A Appendix

A.1 Primary- and Secondary antibodies used in PSC activation study

Table 1: Primary- and Secondary antibodies used in PSC activation study

	Antibody	Source	Clonality	Isotype	Dilution	Company
Primary	α-SMA	Mouse	Monoclonal	IgG	1:400	Sigma-Aldrich (St. Louis, MO, USA)
	YAP	Mouse	Monoclonal	IgG	1:100	Santa Cruz Biotechnology Inc. (Dallas, TX, USA)
	ITGA5	Goat	Monoclonal	IgG	1:100	RD Systems Inc. (Minneapolis, MN, USA)
Secondary	Anti-mouse Alexa Fluor 488	Donkey	Monoclonal	IgG	1:100	Thermo Fisher Scientific Inc. (Waltham, MA, USA)
	Anti-mouse Alexa Fluor 594	Goat	Monoclonal	IgG	1:100	Thermo Fisher Scientific Inc. (Waltham, MA, USA)
	Anti-goat Alexa Fluor 488	Donkey	Monoclonal	IgG	1:100	Thermo Fisher Scientific Inc. (Waltham, MA, USA)

A.2 Immunofluorescence staining plastic well plate

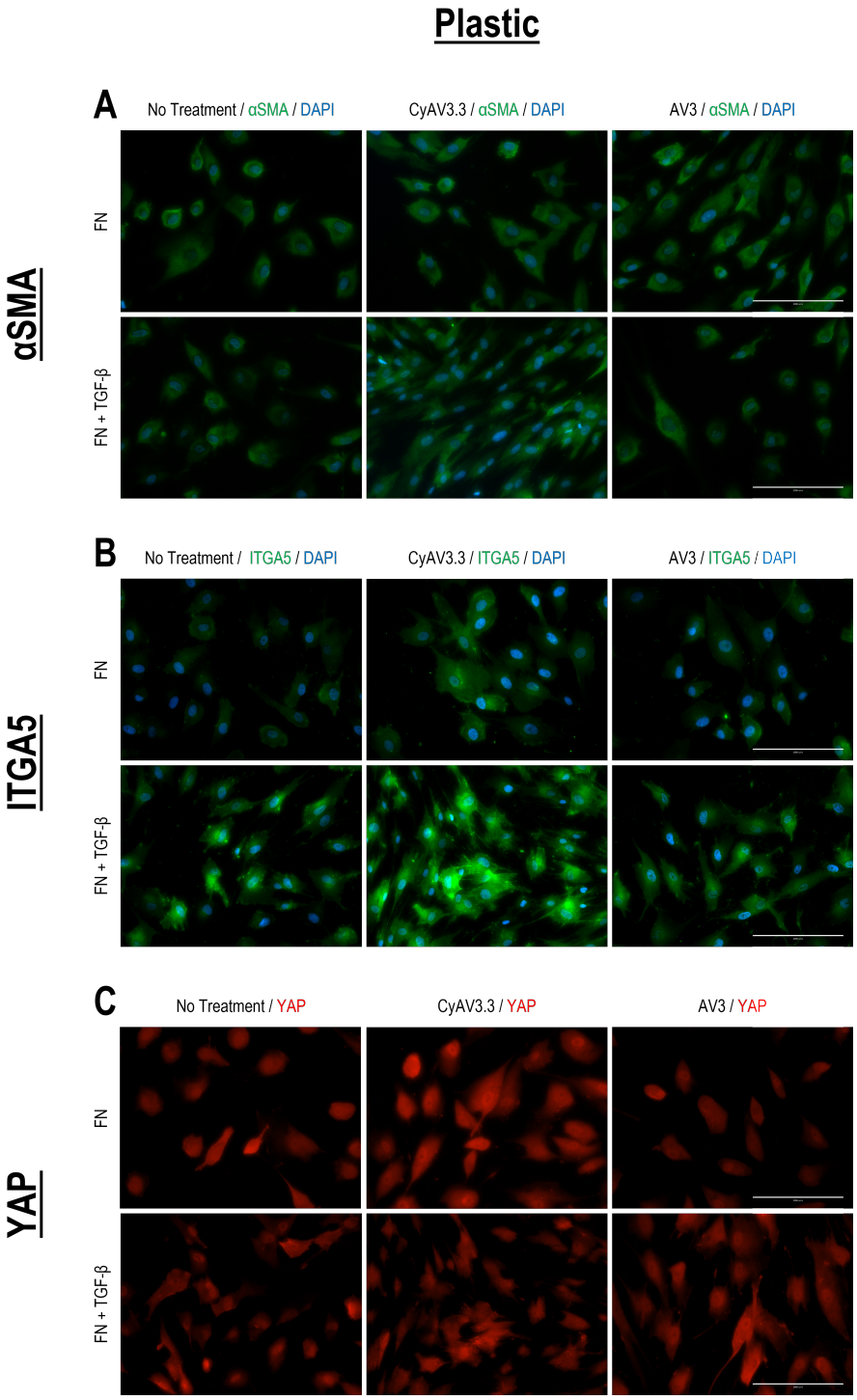

Figure 6: Immunofluorescence staining of PSCs on plastic well plate after 72h of culture. Magnification = 20x ; Scale bar = 200 μm. **(A):** Staining for mouse anti-αSMA monoclonal IgG (Green) and DAPI (Blue) showing αSMA intensity levels. (n=1). **(B):** Staining for goat anti-ITGA5 monoclonal IgG (Green) and DAPI (Blue) showing ITGA5 intensity levels. (n=2). **(C):** Immunofluorescence staining for mouse anti-YAP monoclonal IgG (Red) showing YAP expression intensity. (n=2).

A.3 Collagen I results

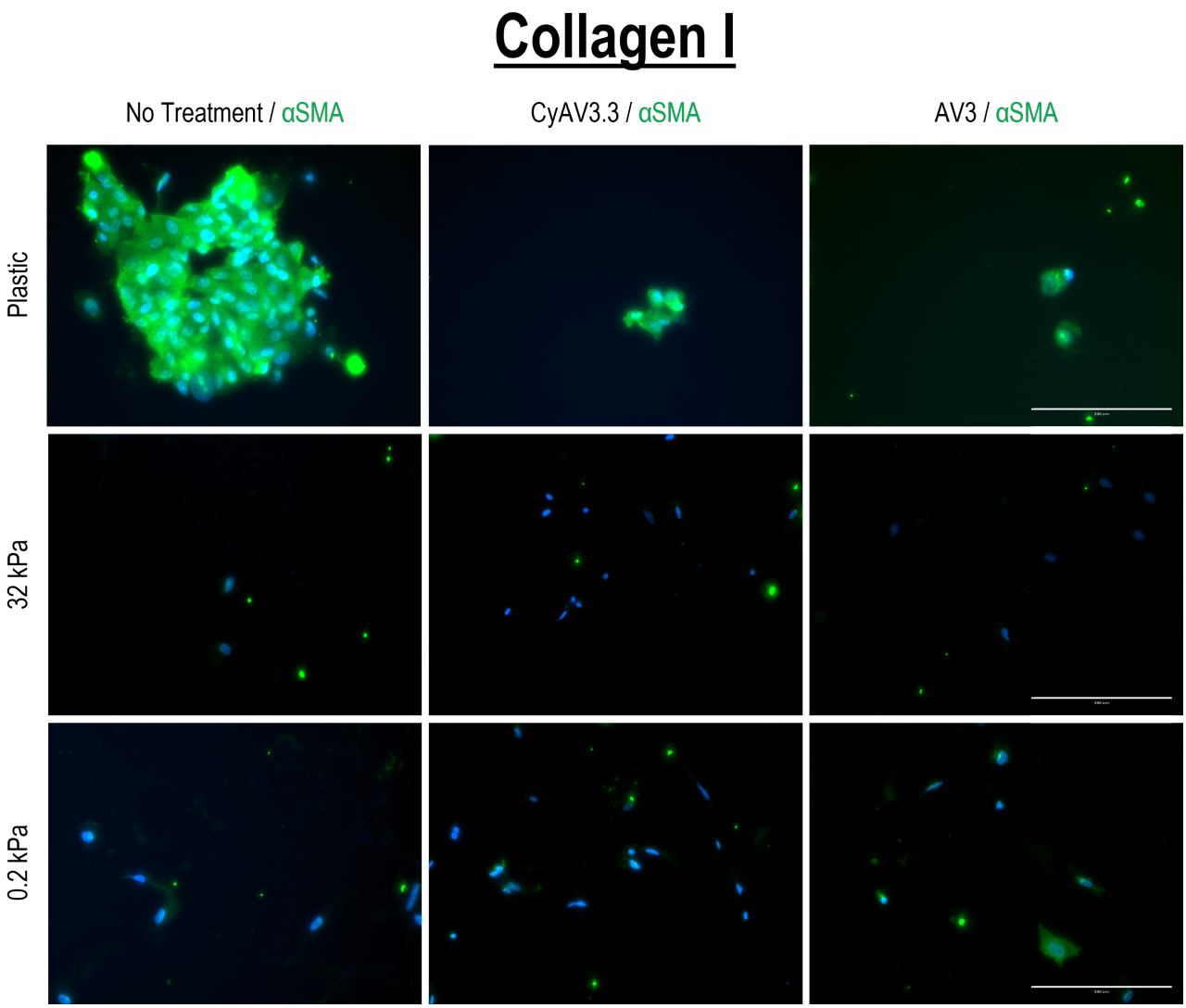

Figure 7: Immunofluorescent staining of PSCs for mouse anti-αSMA monoclonal IgG (Green) and DAPI (Blue) on collagen I coated wells after 72h of culture (n=1). Magnification = 20x ; Scale bar = 200 μm.

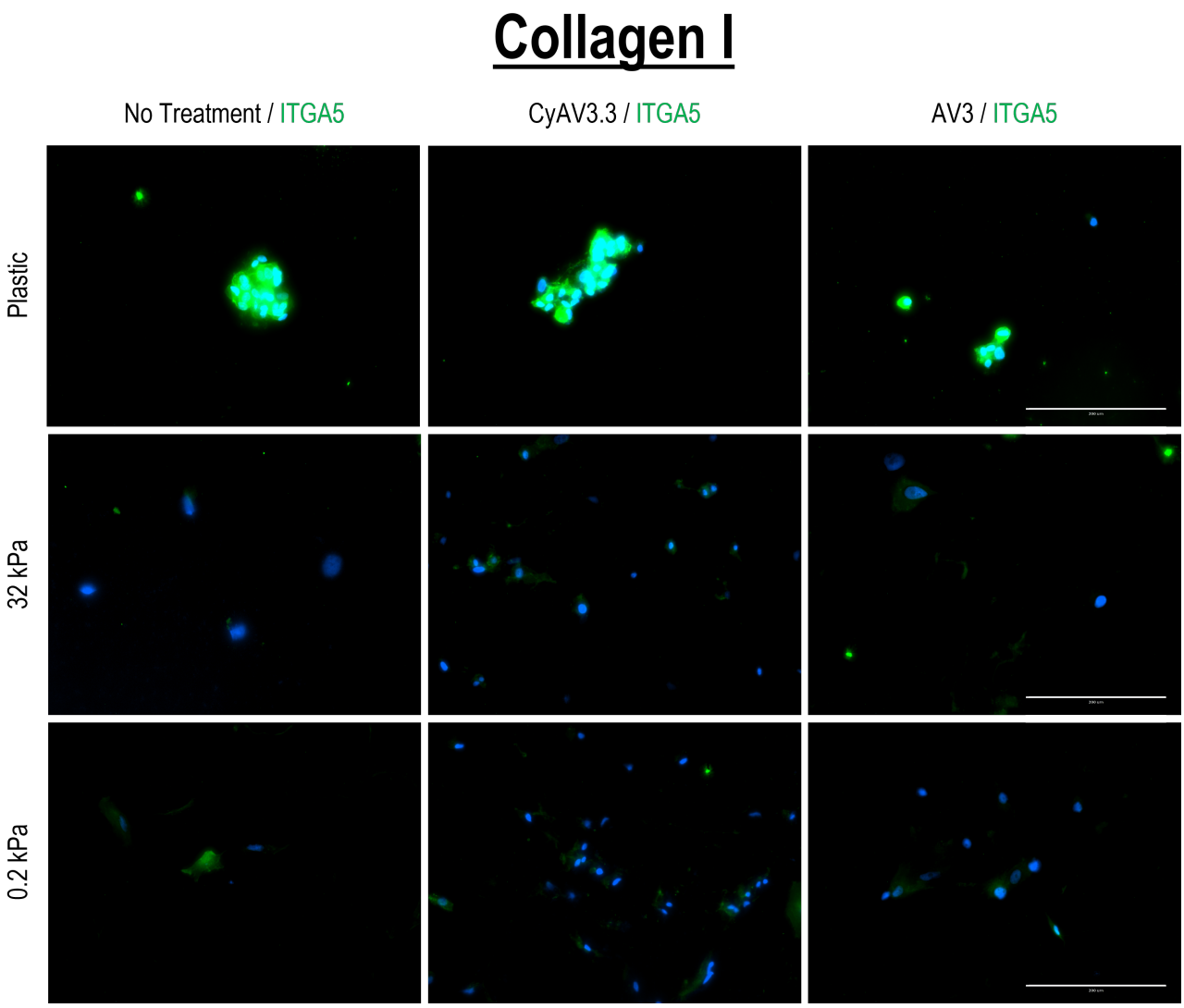

Figure 8: Immunofluorescent staining of PSCs for goat anti-ITGA5 monoclonal IgG (Green) and DAPI (Blue) on collagen I coated wells after 72h of culture (n=2). Magnification = 20x ; Scale bar = 200 μm.

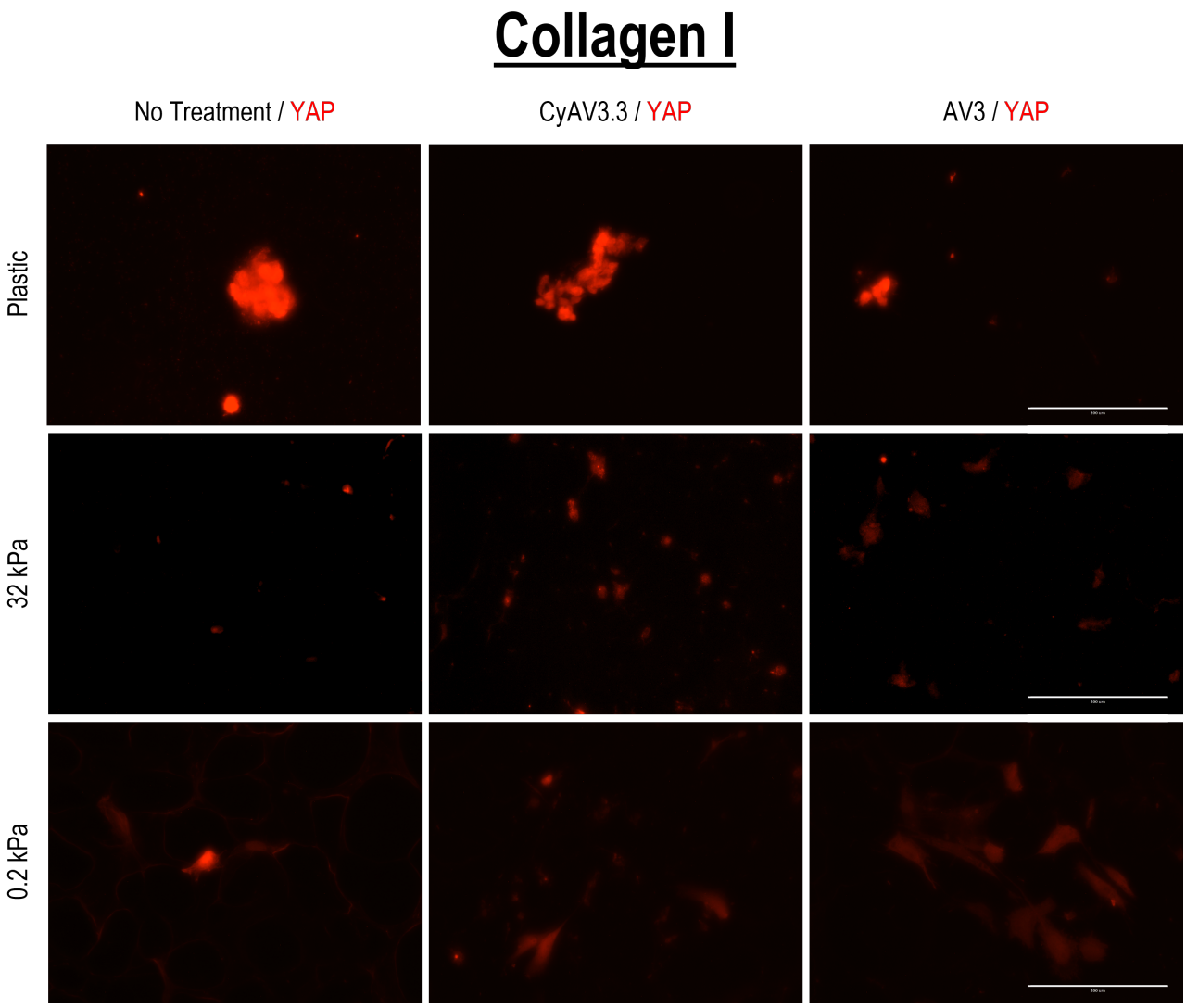

Figure 9: Immunofluorescent staining of PSCs for mouse anti-YAP monoclonal IgG (Red) on collagen I coated wells after 72h of culture (n=2). Magnification = 20x ; Scale bar = 200 μm.